Constrained Tensor Modeling Approach to Blind Multiple-Antenna CDMA Schemes

André L. F. de Almeida, Gérard Favier, and João Cesar M. Mota

***Abstract*—In this paper, we consider an uplink multiple-antenna code-division multiple-access (CDMA) system linking several multiple-antenna mobile users to one multiple-antenna base station. For this system, a constrained third-order tensor decomposition is introduced for modeling the multiple-antenna transmitter as well as the received signal. The constrained structure of the proposed tensor decomposition is characterized by two constraint matrices that have a meaningful physical interpretation in our context. They can be viewed as *canonical allocation matrices* that define the allocation of users' data streams and spreading codes to the transmit antennas. The distinguishing features of the proposed tensor modeling with respect to the already existing tensor-based CDMA models are: i) it copes with multiple transmit antennas and spreading codes per user and ii) it models several spatial spreading/multiplexing schemes with multiple spreading codes by controlling the constrained structure of the tensor signal model. A systematic design procedure for the canonical allocation matrices leading to a unique blind symbol (or joint blind symbol-code) recovery is proposed which allows us to derive a finite set of multiple-antenna schemes for a fixed number of transmit antennas. Identifiability of the proposed tensor model is discussed, and a blind multiuser detection receiver based on the alternating least squares algorithm is considered for performance evaluation of several multiple-antenna CDMA schemes derived from the constrained modeling approach.**

***Index Terms*—Blind detection, canonical allocation, code-division multiple-access (CDMA) systems, constrained tensor modeling, multiple-antenna schemes, spatial multiplexing, spatial spreading.**

I. Introduction

It is well known that the use of multiple antennas at both the transmitter and receiver is promising since it potentially provides increased spectral efficiencies compared to traditional systems employing multiple antennas at the receiver only [1]. In the context of current and upcoming wireless communication standards, the integration of multiple-antenna and code-division multiple access (CDMA) technologies has been the subject of several studies [2]. Spatial multiplexing strategies in conjunction with CDMA is addressed in a few recent works [3]–[5] with focus on layered space-time processing. In [3], the multiple transmit antennas are organized in groups and a unique spreading code is allocated within the same group. The separation of the different groups at the receiver is done by using a layered space-time algorithm [6]. Focusing on the downlink reception, [4] also considers the spatial reuse of the spreading codes and proposes a chip-level equalizer at the receiver to handle the loss of code orthogonality. A space-time receiver for block-spread multiple-antenna CDMA is proposed in [5]. In this case, block-despreading is used prior to space-time filtering in order to eliminate multiuser interference and reduce receiver complexity. On the other hand, CDMA-based transmit diversity schemes have been proposed earlier in [7] and [8] and recently in [9]. These methods, commonly called *space-time spreading*, are capable of providing maximum transmit diversity gain without using extra spreading codes and without an increased transmit power. However, space-time spreading methods put more emphasis on diversity than on multiple-access interference. A recent work [10] investigates the performance of a range of linear single-user and multiuser detectors for multiple-antenna CDMA schemes with space-time spreading. In practice, due to the joint presence of multiple-access interference and time-dispersive multipath propagation, the large number of parameters to be estimated at the receiver (e.g., users' multipath channels, received powers, spreading codes) may require too much processing/training overhead and degrade receiver performance.

In a seminal paper [11], the problem of uplink multiuser detection/separation is linked to a parallel factor (PARAFAC) tensor model. It is shown that each received signal sample associated with a receive antenna, a symbol and a chip, can be interpreted as an element of a three-way array, or *third-order tensor*. Using this interpretation, [11] shows that the use of tensor modeling allows the receiver to fully exploit three forms of diversity (time, space, and code) for blind recovering the transmitted symbols/channel/codes, thanks to the powerful uniqueness property of this tensor model which is not shared by matrix models. Generalizations of the classical PARAFAC-based CDMA model were proposed in subsequent works [12]–[16], under different assumptions concerning the multipath propagation structure (e.g., including frequency-selectivity and specular multipath). However, all these works are limited to single-antenna transmissions.

The use of tensor decompositions for modeling multiple-antenna transmissions is proposed in [17]–[20]. A multiantenna scheme based on a tensor modeling is proposed in [17]. Despite its diversity-rate flexibility and built-in identifiability, this multiple-antenna scheme relies only on temporal spreading of

Manuscript received March 13, 2007; revised October 22, 2007. The associate editor coordinating the review of this manuscript and approving it for publication was Prof. Mariane R. Petraglia. The work of A. L. F. de Almeida was supported by the CAPES/Brazil.

A. L. F. de Almeida and G. Favier are with the I3S Laboratory, University of Nice Sophia Antipolis (UNSA), Centre National de la Recherche Scientifique (CNRS), Les Algorithmes/Euclide B, 06903, Sophia Antipolis, Cedex France (e-mail: lima@i3s.unice.fr; favier@i3s.unice.fr).

J. C. M. Mota is with the Wireless Telecom Research Group, Department of Teleinformatics Engineering, Federal University of Ceará, 60455-760, Fortaleza, Ceará, Brazil (e-mail: mota@gtel.ufc.br).

Digital Object Identifier 10.1109/TSP.2008.917028

the data streams (as in a conventional CDMA system). Since there is no spatial spreading of the data streams across the transmit antennas, no transmit spatial diversity is obtained. In [18], a generalized tensor model is proposed for multiple-antenna CDMA systems with blind detection. However, this modeling approach only considers spatial multiplexing. In summary, the common characteristic of the tensor modeling approaches of [17] and [18] is that the number of data streams are restricted to be equal to the number of transmit antennas. The approach of [19] adds some flexibility at the transmitter by allowing the number of data streams to be different from the number of transmit antennas. As opposed to [17] and [18], full spatial spreading of each data stream across the transmit antennas is also permitted. It is shown that the corresponding tensor model has a fixed constrained structure that uniquely depends on the number of data streams and transmit antennas.

This paper presents a new modeling approach for uplink multiple-antenna CDMA schemes with blind multiuser detection. A constrained third-order tensor decomposition is introduced as a mathematical tool for modeling multiple-antenna CDMA schemes with multiple spreading codes. We show that several multiple-antenna schemes ranging from full transmit diversity to full spatial multiplexing and using different patterns of spatial reuse of the spreading codes can be modeled with the aid of two *constraint matrices* formed by canonical vectors. Physically, these matrices act as *canonical allocation matrices* defining the allocation of users' data streams and spreading codes to their transmit antennas. The distinguishing features of the proposed tensor model with respect to the existing tensor-based CDMA models can be briefly summarized as follows.

- The constraints in the tensor model allow to cope with multiple transmit antennas and spreading codes per user or per data-stream, which provides an extension of [17]–[19] where each data stream is associated with only one spreading code.
- Several multiple-antenna schemes with varying degree of spatial spreading, spatial multiplexing, and spreading code reuse can be obtained by adjusting the constraint matrices of the tensor signal model accordingly.

A design procedure for the canonical allocation matrices leading to a unique blind symbol recovery (or, possibly, joint blind symbol-code recovery) is proposed for deriving finite sets of multiple-antenna schemes with a fixed number of transmit antennas. Identifiability of the proposed tensor model is discussed, and a blind joint detection receiver based on the alternating least squares algorithm is considered for performance evaluation of several multiple-antenna CDMA schemes.

It is worth mentioning that constrained tensor models has been an active research topic in other disciplines such as chemometrics [21]–[23]. Most of these works adopt a different interpretation of the constrained structure, by considering Tucker models [24] with constrained core tensor. Uniqueness is generally studied directly from the pattern of zeros of the core tensor. The "PARALIND" model, recently proposed for data analysis in the context of chemometrics problems [25], is probably the most related to our tensor model. This model also makes use of constraint matrices to model the dependence between columns of component matrices.

This paper is organized as follows. After presenting the basic notations used in this work, Section II defines the constrained tensor decomposition. Section III describes the basic system model. The proposed multiple-antenna CDMA model is presented in Section IV and linked to the constrained tensor decomposition. In Section V, the structure of the canonical allocation matrices of the tensor model is detailed and a design procedure for these matrices leading to a unique blind symbol recovery is described. In Section VI, some identifiability issues of the proposed model are discussed, and a blind receiver using an alternating least squares algorithm is proposed. Simulation results are presented in Section VII and the paper is concluded in Section VIII.

Notations: Scalar variables are denoted by lower-case letters $(a, b, \ldots, \alpha, \beta, \ldots)$, vectors are written as boldface lower-case letters $(\mathbf{a}, \mathbf{b}, \ldots, \boldsymbol{\alpha}, \boldsymbol{\beta}, \ldots)$, matrices correspond to boldface capitals $(\mathbf{A}, \mathbf{B}, \ldots)$, and tensors are written as calligraphic letters $(\mathcal{A}, \mathcal{B}, \ldots)$. $\mathbf{A}^T$, $\mathbf{A}^{-1}$, and $\mathbf{A}^{\dagger}$ stand for transpose, inverse and pseudoinverse of $\mathbf{A}$, respectively. $\mathbf{A}^{-T}$ denotes the inverse of the transpose of $\mathbf{A}$. The operator $\mathrm{diag}(\mathbf{a})$ forms a diagonal matrix from its vector argument; $\mathrm{blockdiag}(\mathbf{A}_1, \ldots, \mathbf{A}_N)$ forms a block-diagonal matrix with N matrix blocks; $D_i(\mathbf{A})$ forms a diagonal matrix holding the ith row of $\mathbf{A}$ on its main diagonal, i.e., $D_i(\mathbf{A}) = \mathrm{diag}(\mathbf{A}_{i\cdot})$. The Kronecker and the Khatri-Rao products are denoted by $\otimes$ and $\diamond$, respectively

$$\mathbf{A} \diamond \mathbf{B} = [\mathbf{A}_{\cdot 1} \otimes \mathbf{B}_{\cdot 1}, \ldots, \mathbf{A}_{\cdot R} \otimes \mathbf{B}_{\cdot R}] = \begin{bmatrix} \mathbf{B} D_1(\mathbf{A}) \\ \vdots \\ \mathbf{B} D_I(\mathbf{A}) \end{bmatrix} \in \mathbb{C}^{IJ \times R} \quad (1)$$

with $\mathbf{A} = [\mathbf{A}_{\cdot 1}, \ldots, \mathbf{A}_{\cdot R}] \in \mathbb{C}^{I \times R}$, $\mathbf{B} = [\mathbf{B}_{\cdot 1}, \ldots, \mathbf{B}_{\cdot R}] \in \mathbb{C}^{J \times R}$.

II. Constrained Tensor Decomposition

In this section, we formulate a constrained tensor decomposition [14] which serves as the basic modeling tool for the considered multiple-antenna CDMA system. The link between this decomposition and the physical parameters of our system model is established in Section IV.

Definition: Let us consider a third-order tensor $\mathcal{X} \in \mathbb{C}^{N_1 \times N_2 \times N_3}$, three component matrices $\mathbf{A}^{(1)} \in \mathbb{C}^{N_1 \times L_1}$, $\mathbf{A}^{(2)} \in \mathbb{C}^{N_2 \times L_2}$, $\mathbf{A}^{(3)} \in \mathbb{C}^{N_3 \times F}$, and two *constraint matrices* $\mathbf{\Psi} \in \mathbb{C}^{L_1 \times F}$ and $\mathbf{\Phi} \in \mathbb{C}^{L_2 \times F}$. A constrained tensor decomposition of $\mathcal{X}$ with F *component combinations* is defined in scalar form as

$$x_{n_1,n_2,n_3} = \sum_{f=1}^{F} \sum_{l_1=1}^{L_1} \sum_{l_2=1}^{L_2} a^{(1)}_{n_1,l_1} a^{(2)}_{n_2,l_2} a^{(3)}_{n_3,f} \psi_{l_1,f} \phi_{l_2,f} \quad \text{with} \quad F \geq \max(L_1, L_2) \quad (2)$$

where x_{n_1,n_2,n_3} is an entry of $\mathcal{X} \in \mathbb{C}^{N_1 \times N_2 \times N_3}$, $a^{(1)}_{n_1,l_1} = [\mathbf{A}^{(1)}]_{n_1,l_1}$, $a^{(2)}_{n_2,l_2} = [\mathbf{A}^{(2)}]_{n_2,l_2}$, $a^{(3)}_{n_3,f} = [\mathbf{A}^{(3)}]_{n_3,f}$, are the entries of the first-mode, second-mode, and third-mode component matrices, respectively. Similarly, $\psi_{l_1,f} = [\mathbf{\Psi}]_{l_1,f}$ and

$\phi_{l_2,f} = [\mathbf{\Phi}]_{l_2,f}$ are, respectively, the entries of the two constraint matrices. The columns of $\mathbf{\Psi}$ and $\mathbf{\Phi}$ are canonical vectors[1] of canonical bases $E^{(L_1)} = \{\mathbf{e}_1^{(L_1)}, \ldots, \mathbf{e}_{L_1}^{(L_1)}\} \in \mathbb{R}^{L_1}$ and $E^{(L_2)} = \{\mathbf{e}_1^{(L_2)}, \ldots, \mathbf{e}_{L_2}^{(L_2)}\} \in \mathbb{R}^{L_2}$, respectively. *The two constraint matrices define the component combination pattern in the composition of the tensor*. Otherwise stated, $\mathbf{\Psi}$ determines the coupling between the columns of $\mathbf{A}^{(1)}$ and $\mathbf{A}^{(3)}$ while $\mathbf{\Phi}$ determines the coupling between the columns of $\mathbf{A}^{(2)}$ and $\mathbf{A}^{(3)}$. It is assumed that $\mathbf{\Psi}$ and $\mathbf{\Phi}$ are both full rank matrices, i.e., $\mathrm{rank}(\mathbf{\Psi}) = L_1$ and $\mathrm{rank}(\mathbf{\Phi}) = L_2$. Note that these assumptions mean that every canonical vector of the basis $E^{(L_1)}$ (respectively, $E^{(L_2)}$) appears at least once as a column of $\mathbf{\Psi}$ (respectively, $\mathbf{\Phi}$). We define $\alpha_{l_1} \in [1, F)$ as the number of component combinations involving the l_1th column of $\mathbf{A}^{(1)}$, i.e., the number of times that the l_1th column of $\mathbf{A}^{(1)}$ contributes in the composition of the tensor $\mathcal{X}$. Similarly, $\beta_{l_2} \in [1, F)$ is the number of component combinations involving the l_2th column of $\mathbf{A}^{(2)}$. α_{l_1} (respectively, β_{l_2}) corresponds to the number of 1's entries at the l_1th (respectively, l_2th) row of $\mathbf{\Psi}$ (respectively, $\mathbf{\Phi}$). We have

$$\mathbf{\Psi}\mathbf{\Psi}^T = \mathrm{diag}(\alpha_1, \ldots, \alpha_{L_1}) = \mathrm{diag}(\boldsymbol{\alpha})$$
$$\mathbf{\Phi}\mathbf{\Phi}^T = \mathrm{diag}(\beta_1, \ldots, \beta_{L_2}) = \mathrm{diag}(\boldsymbol{\beta}) \tag{3}$$

where $\boldsymbol{\alpha} = [\alpha_1, \ldots, \alpha_{L_1}]$ and $\boldsymbol{\beta} = [\beta_1, \ldots, \beta_{L_2}]$ are the *component combination vectors* of matrices $\mathbf{A}^{(1)}$ and $\mathbf{A}^{(2)}$, respectively. These vectors satisfy the following constraint:

$$\sum_{l_1=1}^{L_1} \alpha_{l_1} = \sum_{l_2=1}^{L_2} \beta_{l_2} = F. \tag{4}$$

As will be shown later, (2) is useful for modeling multiple-antenna CDMA systems with multiple spreading codes and data streams per user.

III. System Model and Assumptions

We consider the uplink of a single cell synchronous multiple-antenna CDMA system with Q active users and spreading factor P. The base-station receiver is equipped with K antennas and the qth user transmits R_q independent data streams using M_q antennas. Multiple spreading codes per user are allowed, and J_q denotes the number of spreading codes associated with the qth user. Each transmitted data stream contains N symbols. The wireless channel is assumed to be constant during N symbol periods. Flat-fading and user-wise independent multipath propagation is considered. The transmit parameter set $\{R_q, M_q, J_q\}$, $q = 1, \ldots, Q$, utilized by the qth user, as well as the number Q of active users are assumed to be known to the base-station receiver. Users' spreading codes are symbol-periodic. We either assume that the base station has perfect knowledge or has no knowledge of these spreading codes. The "unknown" spreading code assumption is valid in scenarii where multipath propagation induces interchip interference (ICI). In this case, the term "spreading code" corresponds to the *effective* spreading code resulting from the convolution of the transmitted spreading code with the multipath channel [26]. We simply adopt the term "spreading code" throughout the paper for simplicity reasons. We distinguish three different types of multiple-antenna CDMA schemes covered by our modeling approach.

- *Full spatial multiplexing*: $1 < R_q = J_q = M_q$. Each data stream is transmitted using a different transmit antenna and a different spreading code (full code multiplexing).
- *Full spatial spreading*: $1 = R_q \leq J_q \leq M_q$. A single data stream is fully spread over all the transmit antennas to achieve spatial transmit diversity. In this case, the number of used spreading codes may vary from one (full code reuse) up to M_q (full code multiplexing).
- *Combined spreading and multiplexing*: $1 < R_q \leq J_q \leq M_q$. Each data stream is spread only across a subset of available transmit antennas. Different data streams are spread across nonoverlapping transmit antennas (no antenna sharing between any two data streams). Combination of code reuse and code multiplexing is permitted in this case.

We are mostly interested in combined spreading and multiplexing transmit schemes, since full multiplexing and spreading can be considered as particular cases of the combined one. The constrained tensor modeling approach covers a wide variety of combined transmit schemes depending on the chosen constrained structure of the model. This is a key feature of our modeling approach as will be clarified later.

IV. Tensor Signal Model

For the multiple-antenna CDMA system described in the previous section, we formulate a new tensor model for the received signal, based on the constrained tensor decomposition defined in Section II. We start with a single-user model for simplicity reasons. Let $h_{k,m}$ be the spatial fading channel gain between the mth transmit antenna and the kth receive antenna, $s_{n,r} \doteq s((r-1)N + n)$ be the nth symbol of the rth data stream, and $c_{p,j}$ be the pth element of the jth spreading code. Let us define $\mathbf{H} \in \mathbb{C}^{K \times M}$, $\mathbf{S} \in \mathbb{C}^{N \times R}$, and $\mathbf{C} \in \mathbb{C}^{P \times J}$ as the channel, symbol, and code matrices, where $h_{k,m} \doteq [\mathbf{H}]_{k,m}$, $s_{n,r} \doteq [\mathbf{S}]_{n,r}$, and $c_{p,j} \doteq [\mathbf{C}]_{p,j}$ are, respectively, the entries of these matrices. We can view the discrete-time baseband version of the noise-free received signal at the nth symbol period, pth chip, and kth receive antenna as a third-order tensor $\mathcal{X} \in \mathbb{C}^{N \times P \times K}$ with the (n, p, k)th element defined as $x_{n,p,k} \doteq x_k((n-1)P + p)$. We propose the following input-output model for the considered multiple-antenna CDMA system:

$$x_{n,p,k} = \sum_{m=1}^{M} u_{n,p,m} h_{k,m} \tag{5}$$

where $u_{n,p,m} \doteq u_m((n-1)P + p)$ is the (n, p, m)th element of the third-order tensor $\mathcal{U} \in \mathbb{C}^{N \times P \times M}$ representing the effective (precoded) transmitted signal. We treat $\mathcal{U}$ as the output of a *constrained space-time spreading* operation, which is modeled by the following constrained tensorial transformation:

$$u_{n,p,m} = \sum_{r=1}^{R} \sum_{j=1}^{J} g_m(r, j) s_{n,r} c_{p,j} \tag{6}$$

[1] A canonical vector $\mathbf{e}_n^{(N)} \in \mathbb{R}^N$ is a unitary vector containing an element equal to 1 in its nth position and 0's elsewhere.

where

$$g_m(r,j) \doteq \psi_{r,m}\phi_{j,m} \tag{7}$$

is the (r,j)th element of $\mathbf{G}_m \in \mathbb{C}^{R\times J}$. This matrix defines the allocation of R data streams and J spreading codes to the mth transmit antenna. Let us define

$$\mathbf{G} = \mathbf{\Psi}\mathbf{\Phi}^T \in \mathbb{C}^{R\times J}$$

as the *stream-to-code allocation matrix*. This matrix synthesizes the constrained structure of the model. It is given by the inner product of two *canonical allocation matrices* $\mathbf{\Psi} \in \mathbb{C}^{R\times M}$ and $\mathbf{\Phi} \in \mathbb{C}^{J\times M}$, respectively. The use of the terminology "canonical allocation" for $\mathbf{\Psi}$ and $\mathbf{\Phi}$ is due to the fact that both matrices are composed of canonical vectors controlling the coupling of R data streams and J spreading codes to M transmit antennas, respectively. $\mathbf{\Psi}$ can be viewed as the *stream-to-antenna allocation matrix* and $\mathbf{\Phi}$ as the *code-to-antenna allocation matrix*.

The physical interpretation of (6) is that each data symbol $s_{n,r}$ is spread up to J times using the spreading codes $c_{p,1},\ldots,c_{p,J}$. Each spread symbol $s_{n,r}c_{p,j}$ is then loaded at the mth transmit antenna. Depending on the structure of the $g_m(r,j)$'s, the same spread symbol $s_{n,r}c_{p,j}$ may simultaneously be loaded at several transmit antennas in order to benefit from transmit spatial diversity. From (5) and (6), we can express the received signal as

$$x_{n,p,k} = \sum_{m=1}^{M}\sum_{r=1}^{R}\sum_{j=1}^{J} g_m(r,j)s_{n,r}c_{p,j}h_{k,m}. \tag{8}$$

By comparing (2) and (8), we can deduce the following correspondences:

$$(N_1,N_2,N_3,L_1,L_2,F) \rightarrow (N,P,K,R,J,M)$$
$$(\mathbf{A}^{(1)},\mathbf{A}^{(2)},\mathbf{A}^{(3)}) \rightarrow (\mathbf{S},\mathbf{C},\mathbf{H}). \tag{9}$$

A. Multiuser Signal Model

Some definitions are now introduced, which allow us to view (8) also as a multiuser signal model. In the multiuser case, $R = R_1+\cdots+R_Q$, $J = J_1+\cdots+J_Q$, and $M = M_1+\cdots+M_Q$ denote, respectively, the total number of data streams, spreading codes, and transmit antennas considered, i.e., summed over all the Q users. In this case, $\mathbf{H}$, $\mathbf{S}$ and $\mathbf{C}$ are interpreted as *aggregate* channel, symbol, and code matrices concatenating Q matrix-blocks, i.e.,

$$\mathbf{H} = \left[\mathbf{H}^{(1)},\ldots,\mathbf{H}^{(Q)}\right] \in \mathbb{C}^{K\times M}$$
$$\mathbf{S} = \left[\mathbf{S}^{(1)},\ldots,\mathbf{S}^{(Q)}\right] \in \mathbb{C}^{N\times R}$$
$$\mathbf{C} = \left[\mathbf{C}^{(1)},\ldots,\mathbf{C}^{(Q)}\right] \in \mathbb{C}^{P\times J} \tag{10}$$

where $h^{(q)}_{k,m_q} \doteq [\mathbf{H}]_{k,\sum_{i=1}^{q-1}M_i+m_q}$, $s^{(q)}_{n,r_q} \doteq [\mathbf{S}]_{n,\sum_{i=1}^{q-1}R_i+r_q}$, and $c^{(q)}_{p,j_q} \doteq [\mathbf{C}]_{p,\sum_{i=1}^{q-1}J_i+j_q}$ define the entries of the qth user channel, symbol and code matrices, respectively. We can also view the aggregate canonical allocation matrices as a block-diagonal concatenation of Q matrix-blocks

$$\mathbf{\Psi} = \mathrm{blockdiag}\left(\mathbf{\Psi}^{(1)},\ldots,\mathbf{\Psi}^{(Q)}\right) \in \mathbb{C}^{R\times M}$$
$$\mathbf{\Phi} = \mathrm{blockdiag}\left(\mathbf{\Phi}^{(1)},\ldots,\mathbf{\Phi}^{(Q)}\right) \in \mathbb{C}^{J\times M} \tag{11}$$

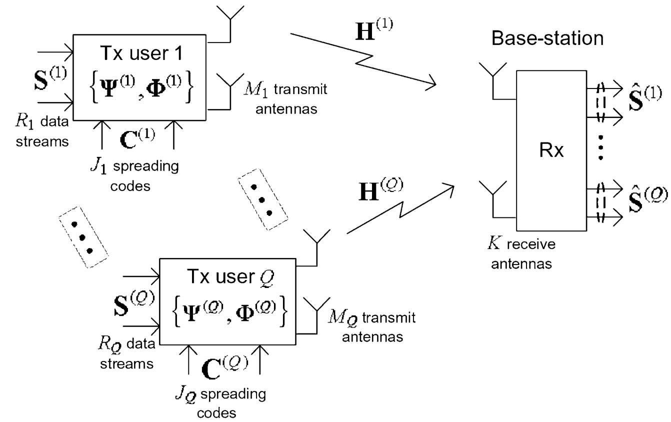

Fig. 1. Uplink model of the proposed multiple-antenna CDMA system.

where $\psi^{(q)}_{r_q,m_q} \doteq [\mathbf{\Psi}^{(q)}]_{r_q,m_q} \doteq [\mathbf{\Psi}]_{\sum_{i=1}^{q-1}R_i+r_q,\sum_{i=1}^{q-1}M_i+m_q}$ and $\phi^{(q)}_{j_q,m_q} \doteq [\mathbf{\Phi}^{(q)}]_{j_q,m_q} = [\mathbf{\Phi}]_{\sum_{i=1}^{q-1}J_i+j_q,\sum_{i=1}^{q-1}M_i+m_q}$ define the entries of the qth user allocation matrices. Similarly, the aggregate coupling matrix is defined as

$$\mathbf{G} = \mathrm{blockdiag}(\mathbf{G}^{(1)},\ldots,\mathbf{G}^{(Q)}) = \mathbf{\Psi}\mathbf{\Phi}^T \in \mathbb{C}^{R\times J}$$
$$\text{with } \mathbf{G}^{(q)} = \mathbf{\Psi}^{(q)}\mathbf{\Phi}^{(q)T}, \quad q=1,\ldots,Q. \tag{12}$$

Fig. 1 depicts the proposed multiple-antenna CDMA model.

B. Matrix Representations

The received signal model (8) can alternatively be expressed in equivalent matrix forms. Let us define $\mathbf{X}_{\cdot\cdot k} \in \mathbb{C}^{N\times P}$ collecting the P chips of the N transmitted symbols associated with the kth receive antenna. $\mathbf{X}_{\cdot\cdot k}$ can be factored in terms of $\mathbf{H}$, $\mathbf{S}$, $\mathbf{C}$, $\mathbf{\Psi}$, and $\mathbf{\Phi}$ as [15]

$$\mathbf{X}_{\cdot\cdot k} = \mathbf{S}\mathbf{\Psi}D_k(\mathbf{H})\mathbf{\Phi}^T\mathbf{C}^T, \quad k=1,\ldots,K. \tag{13}$$

We can also define two other matrices $\mathbf{X}_{n\cdot\cdot} \in \mathbb{C}^{P\times K}$ collecting the received signal samples over P chips and K receive antennas associated with the nth transmitted symbol, and $\mathbf{X}_{\cdot p\cdot} \in \mathbb{C}^{K\times N}$ collecting the received signal samples over N symbol periods and K receive antennas associated with the pth chip of the spreading code. These matrices can be, respectively, factored as

$$\mathbf{X}_{n\cdot\cdot} = \mathbf{C}\mathbf{\Phi}D_n(\mathbf{S}\mathbf{\Psi})\mathbf{H}^T \tag{14}$$
$$\mathbf{X}_{\cdot p\cdot} = \mathbf{H}D_p(\mathbf{C}\mathbf{\Phi})\mathbf{\Psi}^T\mathbf{S}^T \tag{15}$$

and we have $[\mathbf{X}_{n\cdot\cdot}]_{p,k} = [\mathbf{X}_{\cdot p\cdot}]_{k,n} = [\mathbf{X}_{\cdot\cdot k}]_{n,p} = x_{n,p,k}$. Using the tensorial terminology, $\{\mathbf{X}_{n\cdot\cdot}\} \in \mathbb{C}^{P\times K}$, $\{\mathbf{X}_{\cdot p\cdot}\} \in \mathbb{C}^{K\times N}$, and $\{\mathbf{X}_{\cdot\cdot k}\} \in \mathbb{C}^{N\times P}$ are called the first-, second-, and third-mode *matrix-slices*, obtained by "slicing" the tensor $\mathcal{X} \in \mathbb{C}^{N\times P\times K}$ along its first, second, and third dimensions, respectively [27]. Fig. 2 illustrates the decomposition of $\mathbf{X}_{\cdot\cdot k}$ as a function of the aggregate symbol/code/channel matrices $\{\mathbf{S},\mathbf{C},\mathbf{H}\}$ and the canonical allocation matrices $\{\mathbf{\Psi},\mathbf{\Phi}\}$. Let us define the three matrices $\mathbf{X}_1 = [\mathbf{X}^T_{\cdot\cdot 1},\ldots,\mathbf{X}^T_{\cdot\cdot K}]^T \in \mathbb{C}^{KN\times P}$, $\mathbf{X}_2 = [\mathbf{X}^T_{\cdot 1\cdot},\ldots,\mathbf{X}^T_{\cdot P\cdot}]^T \in \mathbb{C}^{PK\times N}$, and $\mathbf{X}_3 = [\mathbf{X}^T_{1\cdot\cdot},\ldots,\mathbf{X}^T_{N\cdot\cdot}]^T \in \mathbb{C}^{NP\times K}$ concatenating the third-mode, second-mode, and first-mode slices of the received signal tensor, respectively, so that $[\mathbf{X}_1]_{(k-1)N+n,p} =$

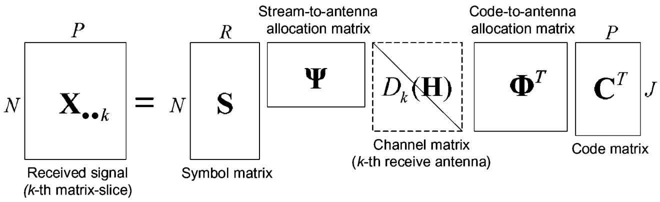

Fig. 2. Constrained decomposition of the received signal tensor (kth matrix slice of the third-mode).

$[\mathbf{X}_2]_{(p-1)K+k,n} = [\mathbf{X}_3]_{(n-1)P+p,k} = x_{n,p,k}$. These matrices are usually called the "unfolded" representations of the signal tensor [27]. Using (1), we get [15]

$$\mathbf{X}_1 = (\mathbf{H} \diamond (\mathbf{S}\boldsymbol{\Psi}))(\mathbf{C}\boldsymbol{\Phi})^T$$
$$\mathbf{X}_2 = ((\mathbf{C}\boldsymbol{\Phi}) \diamond \mathbf{H})(\mathbf{S}\boldsymbol{\Psi})^T$$
$$\mathbf{X}_3 = ((\mathbf{S}\boldsymbol{\Psi}) \diamond (\mathbf{C}\boldsymbol{\Phi}))\mathbf{H}^T. \qquad (16)$$

Relation to the PARAFAC Model of [11]: The parallel can be made by assuming $\{R_q\} = \{J_q\} = \{M_q\} = 1$. In this case, the correspondences between both tensor signal models are $(M, R, J) \rightarrow (Q, Q, Q)$, and we have $\boldsymbol{\Psi} = \boldsymbol{\Phi} = \mathbf{I}_Q$, meaning that the noiseless received signal model reduces to a single-antenna CDMA tensor model [11]

$$x_{n,p,k} = \sum_{q=1}^{Q} s_{n,q} c_{p,q} h_{k,q}. \qquad (17)$$

Therefore, the proposed model can be viewed as a generalization of the one in [11], which is restricted to the single-antenna CDMA case. The introduction of $\boldsymbol{\Psi}$ and $\boldsymbol{\Phi}$ gives flexibility (and more degrees of freedom) to our tensor signal modeling, in the sense that it models CDMA systems with multiple transmit antennas, multiple data streams and multiple spreading codes per user.

Remark 1: This constrained tensor model has properties similar to those of the tensor model proposed in [12] for blind single-antenna CDMA systems with large delay spread. This model can be also viewed as a constrained tensor model where the constrained structure is fixed and intrinsic to the propagation channel (and not to the multiple-antenna transmitter design as in our context).

Illustrative Example: In order to illustrate the physical meaning of the canonical allocation matrices, let us consider the simple example of a single-user multiple-antenna system ($Q = 1$). Assume that the serial input stream is divided into $R = 2$ parallel data streams transmitted by $M = 4$ transmit antennas using $J = 3$ orthogonal spreading codes. Suppose that the canonical allocation scheme is defined by the following constraint matrices:

$$\boldsymbol{\Psi} = \begin{bmatrix} 1 & 1 & 0 & 0 \\ 0 & 0 & 1 & 1 \end{bmatrix}, \quad \boldsymbol{\Phi} = \begin{bmatrix} 1 & 1 & 0 & 0 \\ 0 & 0 & 1 & 0 \\ 0 & 0 & 0 & 1 \end{bmatrix}. \qquad (18)$$

The unitary entries in the first row of the stream-to-antenna allocation matrix $\boldsymbol{\Psi}$ means that the first data stream is spread across the first and second transmit antennas. Likewise, the second row of $\boldsymbol{\Psi}$ shows that the second data stream is spread across the third and fourth transmit antennas. Now, looking at the code-to-antenna matrix $\boldsymbol{\Phi}$, we can see that the first two antennas share the same spreading code for transmission while the third and fourth transmit antennas are associated with different spreading codes. Several canonical allocation structures with different allocation patterns involving data streams and spreading codes for an arbitrary number of transmit antennas can be accommodated in our tensor model. However, the question is whether or not the chosen structure guarantees the uniqueness of the parameters of interest which are the symbol matrix and, possibly, the code matrix. In the next section, the design of the allocation matrices is studied.

V. Design of the Canonical Allocation Matrices

In this section, we study the design of the canonical allocation matrices for ensuring blind symbol recovery (i.e., uniqueness of $\mathbf{S}$). The construction of the canonical allocation matrices satisfying a proposed design criterion is presented. Then, we describe a procedure for designing $\boldsymbol{\Psi}$ and $\boldsymbol{\Phi}$ which allows us to derive a family of multiple-antenna schemes for a fixed number of transmit antennas.

A. Generating Vectors

For simplicity reasons, we omit the user-dependent index q in the design of the canonical allocation matrices by considering a single-user system. Since the design criterion for these matrices is exactly the same for all the users, we can bypass the user-dependent notation without loss of generality while simplifying the notation.

We propose to parameterize the two canonical allocation matrices by their *generating vectors*. Let us define $\boldsymbol{\alpha} = [\alpha_1, \ldots, \alpha_R]$ and $\boldsymbol{\beta} = [\boldsymbol{\beta}_1, \ldots, \boldsymbol{\beta}_R]$, where $\boldsymbol{\beta}_r = [\beta_{r,1}, \ldots, \beta_{r,J_r}]$, as the generating vectors of $\boldsymbol{\Psi}$ and $\boldsymbol{\Phi}$, respectively. These vectors completely characterize the canonical allocation structure in the considered multiple-antenna system. Note the following:

- α_r is the rth *spatial spreading factor*, and denotes the number of transmit antennas associated with the rth data stream;
- β_{r,j_r} is the j_rth *code reuse factor*, and denotes the number of transmit antennas using the j_rth spreading code of the rth data stream, $j_r = 1, \ldots, J_r$.

The generating vectors $\boldsymbol{\alpha}$ and $\boldsymbol{\beta}$ correspond to those defined in (3) for the constrained tensor decomposition. By analogy with (4), we have the following correspondences $(l_1, l_2) \rightarrow (r, j)$, $(L_1, L_2) \rightarrow (R, J)$ and $F \rightarrow M$, yielding the following constraint:

$$\sum_{r=1}^{R} \alpha_r = \sum_{r=1}^{R} \sum_{j_r=1}^{J_r} \beta_{r,j_r} = M \qquad (19)$$

i.e., the sum of the elements of $\boldsymbol{\alpha} = [\alpha_1, \ldots, \alpha_R]$ is equal to that of $\boldsymbol{\beta} = [\boldsymbol{\beta}_1, \ldots, \boldsymbol{\beta}_R]$ which is always equal to the number of transmit antennas.

B. Design Criterion

We borrow some basic concepts from partition theory [28] in order to design the canonical allocation matrices. Specifically, the generating vectors $\boldsymbol{\alpha}$ and $\boldsymbol{\beta}$ are interpreted here as *partitions* of size M and dimensions R and J, respectively. The fact that $\boldsymbol{\alpha}$ and $\boldsymbol{\beta}$ are partitions of the same size is due to (19). Physically, $\boldsymbol{\alpha}$ is a partition of M transmit antennas into R subsets transmitting *different* data streams (i.e., the rth data stream is spread across α_r antennas). Likewise, $\boldsymbol{\beta}$ is a partition of M transmit antennas into J subsets, each one of which is associated with a *different* code (i.e., the jth code is reused by β_j antennas). We suppose that $\boldsymbol{\alpha}$ and $\boldsymbol{\beta}$ satisfy the following design criterion:

$$\sum_{j_r=1}^{J_r} \beta_{r,j_r} = \|\boldsymbol{\beta}_r\|_1 = \alpha_r, \quad 1 \le r \le R \tag{20}$$

where J_r is the dimension of the rth subpartition $\boldsymbol{\beta}_r = [\beta_{r,1}, \ldots, \beta_{r,J_r}]$ of $\boldsymbol{\beta}$, with $J_1 + \cdots + J_R = J$. β_{r,j_r} corresponds to the number of times the j_rth spreading code is reused within the rth antenna set, while J_r corresponds to the number of different spreading codes within the rth antenna set.

Based on (20), we propose the following partitioned construction for $\boldsymbol{\Psi}$ and $\boldsymbol{\Phi}$:

$$\begin{aligned} &\boldsymbol{\Psi} = [\boldsymbol{\Psi}_1, \ldots, \boldsymbol{\Psi}_r, \ldots, \boldsymbol{\Psi}_R] \\ \text{with} \quad &\boldsymbol{\Psi}_r = \mathbf{1}_{\alpha_r}^T \otimes \mathbf{e}_r^{(R)} \in \mathbb{R}^{R \times \alpha_r}, \quad r = 1, \ldots, R \end{aligned} \tag{21}$$

and

$$\begin{aligned} &\boldsymbol{\Phi} = [\boldsymbol{\Phi}_1, \ldots, \boldsymbol{\Phi}_r, \ldots, \boldsymbol{\Phi}_R] \\ \text{with} \quad &\boldsymbol{\Phi}_r = [\boldsymbol{\Phi}_{r,1}, \ldots, \boldsymbol{\Phi}_{r,j_r}, \ldots, \boldsymbol{\Phi}_{r,J_r}] \in \mathbb{R}^{J \times \alpha_r} \\ \text{and} \quad &\boldsymbol{\Phi}_{r,j_r} = \begin{bmatrix} \mathbf{0}_{\bar{J}_{r-1} \times \beta_{r,j_r}} \\ \mathbf{1}_{\beta_{r,j_r}}^T \otimes \mathbf{e}_{j_r}^{(J_r)} \\ \mathbf{0}_{(J-\bar{J}_r) \times \beta_{r,j_r}} \end{bmatrix} \in \mathbb{R}^{R \times \beta_{r,j_r}} \end{aligned} \tag{22}$$

where $\mathbf{1}_n = [1, 1, \ldots, 1]^T$ is an n-dimensional vector of ones, and $\bar{J}_r = \sum_{i=1}^{r} J_i$. Note that $\boldsymbol{\Psi}_r$ is the canonical allocation matrix associated with the rth transmitted data stream, and $\boldsymbol{\Phi}_{r,j_r}$ is the canonical allocation matrix associated with the j_rth spreading code used by the rth data stream.

Practical Implications of the Proposed Design Criterion: The proposed design criterion for determining the structure of $\boldsymbol{\Psi}$ and $\boldsymbol{\Phi}$ from $\boldsymbol{\alpha}$ and $\boldsymbol{\beta}$, respectively, has some practical implications. First, we can observe that the spatial spreading of the data streams and the reuse of the spreading codes are restricted to adjacent transmit antennas only. This restriction can easily be deduced from the repetition pattern of identical canonical vectors in these matrices. Another implication of this construction is that different data streams cannot be associated with the same spreading code for transmission. In other words, spreading code reuse only takes place across the transmit antennas transmitting the same data stream.

Constructing $\boldsymbol{\Psi}(\boldsymbol{\alpha})$ and $\boldsymbol{\Phi}(\boldsymbol{\beta})$ according to the design criterion (20), we can verify (see the Appendix) that any $\tilde{\mathbf{S}}$ and $\tilde{\mathbf{C}}$ satisfying the model are related to $\mathbf{S}$ and $\mathbf{C}$, respectively, by

$$\begin{aligned} \tilde{\mathbf{S}} &= \mathbf{S}\mathbf{T}, \quad \mathbf{T} = \mathrm{diag}(t_1, \ldots, t_R)\boldsymbol{\Pi}_R \\ \tilde{\mathbf{C}} &= \mathbf{C}\mathbf{U}, \quad \mathbf{U} = \mathrm{blockdiag}(\mathbf{U}_1, \ldots, \mathbf{U}_R)\bar{\boldsymbol{\Pi}}_J \end{aligned} \tag{23}$$

where $\mathbf{U}_r \in \mathbb{C}^{J_r \times J_r}$ is a nonsingular transformation ambiguity matrix, $\boldsymbol{\Pi}_R \in \mathbb{R}^{R \times R}$ is a permutation matrix and $\bar{\boldsymbol{\Pi}}_J \in \mathbb{R}^{J \times J}$ is a block-diagonal permutation matrix. In other words, the symbol matrix $\mathbf{S}$ is unique up to column permutation and scaling while the code matrix $\mathbf{C}$ is unique up to a multiplication by a nonsingular block-diagonal matrix and column permutation. It is worth noting that the simultaneous uniqueness of $\mathbf{S}$ and $\mathbf{C}$ up to permutation and scaling arises in a particular case of (20) where $R = J$ and $\alpha_r = \beta_r$, $r = 1, \ldots, R$.

TABLE I
SET OF SCHEMES FOR $M = 4$

(R, J)	$\boldsymbol{\alpha}$'s	$\boldsymbol{\beta}$'s	nb. of schemes
(1, 1)	4	4	1
(1, 2)	4	{[3 1]; [2 2]}	2
(1, 3)	4	[2 1 1]	1
(1, 4)	4	[1 1 1 1]	1
(2, 2)	{[3 1]; [2 2]}	{[3 1]; [2 2]}	2
(2, 3)	{[3 1]; [2 2]}	[2 1 1]	2
(2, 4)	{[3 1]; [2 2]}	[1 1 1 1]	2
(3, 3)	[2 1 1]	[2 1 1]	1
(3, 4)	[2 1 1]	[1 1 1 1]	1
(4, 4)	[1 1 1 1]	[1 1 1 1]	1

Remark 2: The uniqueness of $\mathbf{S}$ is the major concern in this paper, since our final goal is the blind recovery of the transmitted data streams. On the other hand, the uniqueness of $\mathbf{H}$ is not required, since we are interested in a "direct" detection without using any knowledge about the channel.

C. Design Procedure

We propose a systematic procedure for building the canonical allocation matrices $\boldsymbol{\Psi}$ and $\boldsymbol{\Phi}$ in (21)–(22) based only on the generating vectors $\boldsymbol{\alpha}$ and $\boldsymbol{\beta}$, according to the following steps:

i) a choice of $\boldsymbol{\alpha}$ is made for a fixed number M of transmit antennas (partition size) and a fixed number R of input data streams (partition dimension);

ii) for every α_r, a sub-partition $\boldsymbol{\beta}_r = [\beta_{r,1}, \ldots, \beta_{r,J_r}]$ of size α_r and dimension J_r is formed so that (20) is satisfied and $\boldsymbol{\beta} = [\boldsymbol{\beta}_1, \ldots, \boldsymbol{\beta}_R]$. The value of J_r, i.e., the number of spreading codes for the rth data stream, is a design parameter;

iii) $\boldsymbol{\Psi}$ and $\boldsymbol{\Phi}$ are built according to (21)–(22).

D. Set of Canonical Allocation Schemes

More than one choice for $\boldsymbol{\beta}$ may be possible for a fixed $\boldsymbol{\alpha}$. This is due to the fact that more than one way of choosing a subpartition $\boldsymbol{\beta}_r$ from α_r, $r = 1 \ldots, R$ may be possible without affecting the uniqueness property of the model. Each choice will lead to a different allocation structure $\mathbf{G} = \boldsymbol{\Psi}(\boldsymbol{\alpha})\boldsymbol{\Phi}(\boldsymbol{\beta})^T$. Following the proposed design procedure, a family of multiple-antenna CDMA schemes can be derived from the different possible choices of $\boldsymbol{\alpha}$ and $\boldsymbol{\beta}$. Table I shows the set of schemes for $M = 4$ transmit antennas. We assume that $\alpha_1 \ge \cdots \ge \alpha_R$, and $\beta_{1,1} \ge \cdots \ge \beta_{1,J_1} \ge \cdots \ge \beta_{R,1} \ge \cdots \ge \beta_{R,J_R}$. This assumption eliminates equivalent (redundant) schemes. For example, an allocation scheme with $\boldsymbol{\alpha} = [1\ 3]$ and $\boldsymbol{\beta} = [1\ 2\ 1]$ is considered equivalent to the one with $\boldsymbol{\alpha} = [3\ 1]$ and $\boldsymbol{\beta} = [2\ 1\ 1]$. Both schemes have the same spreading and multiplexing pattern (the order of association of data streams and spreading codes with the transmit antennas is irrelevant), and have the same uniqueness property [both schemes satisfy (20)]. In this table, the different schemes are listed according to increasing values of R and J.

It can be seen from this table that 14 allocation schemes are possible. Note that for some values of R and J, two schemes exist. Let us consider the case $(R, J) = (1, 2)$, where we have two possible choices. For $\boldsymbol{\beta} = [3\ 1]$, antennas 1, 2, and 3 use the same spreading code, which is different from the one used by antenna 4. On the other hand, for $\boldsymbol{\beta} = [2\ 2]$ each spreading code is used twice by two different antenna sets. Both are full spatial spreading schemes, but having different code reuse patterns. For $(R, J) = (2, 2)$, we have two feasible schemes, and they correspond to those satisfying $\boldsymbol{\alpha} = \boldsymbol{\beta}$. For $(R, J) = (2, 3)$ and $(2, 4)$ we also have two schemes. Note that the basic difference between the schemes $(R, J) = (2, 2)$, $(2, 3)$ and $(2, 4)$ is on the code reuse/multiplexing pattern, the spatial spreading pattern being the same.

E. Discussion

In practice, $\boldsymbol{\Psi}$ and $\boldsymbol{\Phi}$ can be designed based on practical restrictions such as the number of available spreading codes and transmit antennas, data-rate, and diversity requirements. One way of optimizing the allocation matrices is to take advantage of *a priori* channel state information at the transmitter. Since our design procedure allows the determination of a finite-set, or codebook, of feasible allocation schemes, limited feedback precoding methods [29], [30] can be used to select the best pair of constraint matrices at the transmitter. Although interesting, performance-oriented optimization of $\boldsymbol{\Psi}$ and $\boldsymbol{\Phi}$ is a topic beyond the scope of this paper and will be elaborated in the future. Here, we only focus on uniqueness aspects for designing the transmit schemes. However, we conjecture that the optimization of the allocation structure can allow substantial performance gains compared to the nonoptimized case. This issue deserves more investigation.

VI. Blind Receiver

As far as multiuser separation/detection is concerned, the goal of the base-station receiver is to separate the Q users' transmissions (symbols/channels/codes) while recovering the data transmitted by each user. In this paper, we consider a joint blind processing without using training sequences or resorting to *a priori* channel knowledge. In this case, model *identifiability* is a fundamental issue to be considered. This issue is now studied.

A. Identifiability

Let us rewrite the three unfolded matrices of the received signal (16) in the following equivalent manner:

$$\begin{aligned}\mathbf{X}_1 &= \mathbf{Z}_1(\mathbf{H}, \mathbf{S})\mathbf{C}^T\\ \mathbf{X}_2 &= \mathbf{Z}_2(\mathbf{C}, \mathbf{H})\mathbf{S}^T\\ \mathbf{X}_3 &= \mathbf{Z}_3(\mathbf{S}, \mathbf{C})\mathbf{H}^T\end{aligned} \tag{24}$$

where

$$\begin{aligned}\mathbf{Z}_1(\mathbf{H}, \mathbf{S}) &= (\mathbf{H} \diamond (\mathbf{S}\boldsymbol{\Psi}))\boldsymbol{\Phi}^T \in \mathbb{C}^{KN \times J}\\ \mathbf{Z}_2(\mathbf{C}, \mathbf{H}) &= ((\mathbf{C}\boldsymbol{\Phi}) \diamond \mathbf{H})\boldsymbol{\Psi}^T \in \mathbb{C}^{PK \times R}\\ \mathbf{Z}_3(\mathbf{S}, \mathbf{C}) &= (\mathbf{S}\boldsymbol{\Psi}) \diamond (\mathbf{C}\boldsymbol{\Phi}) \in \mathbb{C}^{NP \times M}\end{aligned} \tag{25}$$

are the three constrained Khatri-Rao factorizations of the received signal model.

Theorem (Identifiability): The identifiability of the constrained tensor model (8) in the least square (LS) sense requires that $\mathbf{Z}_1(\mathbf{H}, \mathbf{S})$, $\mathbf{Z}_2(\mathbf{C}, \mathbf{H})$, and $\mathbf{Z}_3(\mathbf{S}, \mathbf{C})$ are full column-rank, which implies

$$KN \geq J, \quad PK \geq R, \quad \text{and} \quad NP \geq M. \tag{26}$$

Proof: The proof follows the same reasoning as the one given in [31] for the PARAFAC model. From (24), $\mathbf{C}$ is identifiable in the LS sense if and only if $\mathbf{Z}_1(\mathbf{H}, \mathbf{S})$ admits a unique left pseudo-inverse, i.e., if it does *not* exist $\mathbf{X} \neq \mathbf{0}_J$ belonging to the kernel $K(\mathbf{Z}_1)$ such that $\mathbf{Z}_1(\mathbf{X} + \mathbf{C}^T) = \mathbf{Z}_1\mathbf{C}^T$, i.e., $K(\mathbf{Z}_1) = \{\mathbf{0}_J\}$. From the rank theorem, we have

$$\dim(K(\mathbf{Z}_1)) = 0 \Rightarrow \text{rank}(\mathbf{Z}_1) = J$$

which means that $\mathbf{Z}_1$ is full column-rank. Moreover, as we have $\text{rank}(\mathbf{Z}_1) \leq \min(KN, J)$, it follows that $KN \geq J$, i.e., $\mathbf{Z}_1$ is tall. Applying the same reasoning to $\mathbf{S}$ and $\mathbf{H}$ in $\mathbf{X}_2 = \mathbf{Z}_2(\mathbf{C}, \mathbf{H})\mathbf{S}^T$ and $\mathbf{X}_3 = \mathbf{Z}_3(\mathbf{S}, \mathbf{C})\mathbf{H}^T$, we obtain the inequalities $PK \geq R$ and $NP \geq M$, respectively. ■

From (26), the following corollaries can be obtained.

1) For $R = J = M$ (equal number of data streams, spreading codes and transmit antennas), the constrained tensor decomposition reduces to the PARAFAC decomposition of M factors, and (26) is equivalent to condition [31]

$$\min(NP, KN, PK) \geq M.$$

2) For $1 < R = J < M$ (equal number of data streams and spreading codes) we can decouple (26) into the two following conditions:

$$K \cdot \min(N, P) \geq R, \quad \text{and} \quad NP \geq M.$$

3) For $1 < R < J = M$ (equal number of spreading codes and transmit antennas), we obtain the two following conditions:

$$N \cdot \min(K, P) \geq M, \quad \text{and} \quad KP \geq R.$$

B. Discussion on the Identifiability Conditions

1) Interpretation of (26): These identifiability conditions relate all the system parameters of interest, which belong either to the transmitted or to the received signal dimensions. The transmitted signal dimensions are (R, J, M) while the receiver dimensions are (N, P, K). These conditions can be interpreted in the following manner. An increase in a transmitted signal dimension (e.g., *data stream*, *spreading code*, or *transmit antenna* dimension), representing an increase in the number of system parameters to be identified at the receiver, must be compensated by an increase in the corresponding received signal dimension(s). As a consequence of tensor modeling, an identifiability tradeoff arises in (26). For instance, an increase in the number R of data streams can be compensated by increasing the number K of receive antennas or the spreading factor P, or both, accordingly. A similar reasoning applies when the number of spreading codes or transmit antennas is increased.

2) K-Rank Based Conditions: Model (16) can be viewed as a third-order PARAFAC model with three equivalent factor matrices $\bar{\mathbf{S}} = \mathbf{S}\boldsymbol{\Psi}$, $\bar{\mathbf{C}} = \mathbf{C}\boldsymbol{\Phi}$ and $\mathbf{H}$. Due to the presence of sets of identical columns in $\boldsymbol{\Psi}$ and $\boldsymbol{\Phi}$, and consequently in $\bar{\mathbf{S}}$ and $\bar{\mathbf{C}}$, the identifiability result of [11], which is based on the concept of k-rank, does not apply to this constrained tensor model. This is due to the fact that $\bar{\mathbf{S}}$ and $\bar{\mathbf{C}}$ have k-rank equal to one, and the sufficient condition of [11] fails (see [11] for further details). The same comment is valid for the PARALIND model of [12] and [25], which exhibits similar constrained structure.

C. Receiver Algorithm

Now, we present the proposed blind receiver algorithm for symbol recovery. In order to exploit the tensor modeling of the received signal, we make use of the alternating least squares (ALS) algorithm [11], [21], which is the classical solution for estimating the component matrices of a tensor model. The ALS algorithm consists in fitting a third-order tensor model to the received data by alternatively minimizing three LS criteria. In our case, the component matrices to be estimated are the symbol, code and channel matrices, while the received data correspond to the noisy signal measured with the receiver antennas.

The ALS algorithm makes use of the three unfolded matrices representing the received signal in (24). We assume that the identifiability conditions (26) are fulfilled. At each step of this algorithm, one component matrix is estimated in the LS sense, while the two others are fixed to their values obtained at the two previous steps. $\mathbf{\Psi}$ and $\mathbf{\Phi}$ are known matrices and are fixed during the iterative estimation process. At the first iteration, $\hat{\mathbf{S}}_{(0)}$ and $\hat{\mathbf{H}}_{(0)}$ are randomly initialized. Assuming unknown spreading codes, the ALS algorithm is composed of three estimation steps.

Define $\tilde{\mathbf{X}}_i = \mathbf{X}_i + \mathbf{V}_i$, $i = 1, 2, 3$, as a noisy version of $\mathbf{X}_i$, where $\mathbf{V}_i$ is an additive complex-valued white Gaussian noise matrix.

1) Set $i = 0$;
   Randomly initialize $\hat{\mathbf{H}}_{(i=0)}$ and $\hat{\mathbf{S}}_{(i=0)}$;
2) $i = i + 1$;
3) Using $\tilde{\mathbf{X}}_1$, find an LS estimate of $\mathbf{C}$:

$$\hat{\mathbf{C}}_{(i)}^T = \left[\mathbf{Z}_1\left(\hat{\mathbf{H}}_{(i-1)}, \hat{\mathbf{S}}_{(i-1)}\right)\right]^{\dagger} \tilde{\mathbf{X}}_1;$$

4) Using $\tilde{\mathbf{X}}_2$, find an LS estimate of $\mathbf{S}$:

$$\hat{\mathbf{S}}_{(i)}^T = \left[\mathbf{Z}_2\left(\hat{\mathbf{C}}_{(i)}, \hat{\mathbf{H}}_{(i-1)}\right)\right]^{\dagger} \tilde{\mathbf{X}}_2;$$

5) Using $\tilde{\mathbf{X}}_3$, find an LS estimate of $\mathbf{H}$:

$$\hat{\mathbf{H}}_{(i)}^T = \left[\mathbf{Z}_3\left(\hat{\mathbf{S}}_{(i)}, \hat{\mathbf{C}}_{(i)}\right)\right]^{\dagger} \tilde{\mathbf{X}}_3;$$

6) Repeat steps 2-5 until convergence.

The convergence of the algorithm at the ith iteration is declared when the error between the true received signal tensor and its version reconstructed from the estimated component matrices does not significantly change between iterations i and $i+1$. The conditional update of each matrix may either improve or maintain but cannot worsen the current fit. It is worth noting, however, that the ALS algorithm strongly depends on the initialization, and convergence to local minima can occur. Specifically, the convergence of this algorithm can sometimes fall in regions of "swamps" during which the convergence speed is very small and the error between two consecutive iterations does not significantly decrease [21].

A more efficient initialization strategy consists in first obtaining an estimation of the column space of $\mathbf{C}$, $\mathbf{S}$ and $\mathbf{H}$ using successive singular value decompositions of $\mathbf{X}_1 \in \mathbb{C}^{KN \times P}$, $\mathbf{X}_2 \in \mathbb{C}^{PK \times N}$ and $\mathbf{X}_3 \in \mathbb{C}^{NP \times K}$, respectively. The estimated matrices are linked to the true ones by nonsingular nonadmissible transformation matrices. They can, however, be used as a starting point of the ALS algorithm. This initialization procedure will probably be more efficient than a random initialization. Convergence of the estimates is rapidly achieved when the spreading code matrix $\mathbf{C}$ is known at the receiver [17]. In this case, the first estimation step is skipped. Assuming known spreading codes, we have observed that the ALS algorithm usually converges to the global minimum within 15–30 iterations for a SNR of 20 dB. In contrast, when considering unknown spreading codes, the convergence can be much slower. It can take hundreds or even thousands of iterations in worst-case situations.

Provided that (20) is satisfied, the ALS algorithm will provide a unique estimation of the symbol matrix $\hat{\mathbf{S}}$ up to column permutation and scaling ambiguities. In order to eliminate the scaling ambiguity, we assume that the first transmitted symbol of each data stream is equal to one, i.e., $\mathbf{S}_{1 \cdot} = [1, 1, \ldots, 1]$. Another approach to eliminate such a scaling ambiguity consists in using differential modulation/detection. Permutation ambiguity is only present when $\mathbf{C}$ is unknown. In this case, we resort to a greedy least squares procedure for matching the columns of $\hat{\mathbf{S}}$ and $\mathbf{S}$, as in [11].

VII. Performance Evaluation

In this section, computer simulation results illustrate the performance of the proposed blind multiple-antenna CDMA schemes using different allocation structures for $M = 2, 3$, and 4. The ALS algorithm described in the previous section is used as the multiuser detection receiver. Two different detection assumptions are considered for performance evaluation.

- *Code-assisted detection*: The spreading code matrix $\mathbf{C}$ is assumed to be *known* at the receiver. Hadamard(P) spreading codes are used in this case.
- *Code-blind detection*: The spreading code matrix $\mathbf{C}$ is assumed to be *unknown* at the receiver as a consequence of multipath delay propagation. The spreading code matrix is generated by convolving the Hadamard(P) code with the considered multipath delay channel [26].

Performance evaluation is based on average bit-error-rate (BER) *versus* signal-to-noise ratio (SNR) plots, obtained by means of Monte Carlo runs. The number of runs vary from 1000 to 5000 depending on the simulated SNR value. The BER curves represent the performance averaged on the R transmitted data streams, except in some figures, where we plot the individual performance of each data stream for a more detailed analysis. At each run, the additive noise power is generated according to the SNR value given by $\mathrm{SNR} = 10\log_{10}(\|\mathbf{X}_1\|_F^2 / \|\mathbf{V}_1\|_F^2)$, the spatial channel gains are drawn from an i.i.d. complex-valued Gaussian generator while the transmitted symbols are drawn from a pseudorandom quaternary phase shift keying (QPSK) sequence.

Our simulations focus on challenging system configurations with a small number of receive antennas and short received data blocks, which is more attractive in practice. We assume $K = 2$ and $N = 10$ throughout the simulations, unless otherwise stated. The most relevant parameters to be considered here are the generating vectors $\boldsymbol{\alpha}$ and $\boldsymbol{\beta}$ of the allocation structure, defining the spatial spreading and code reuse factors, respectively. In all the simulations, the transmit parameters are shown

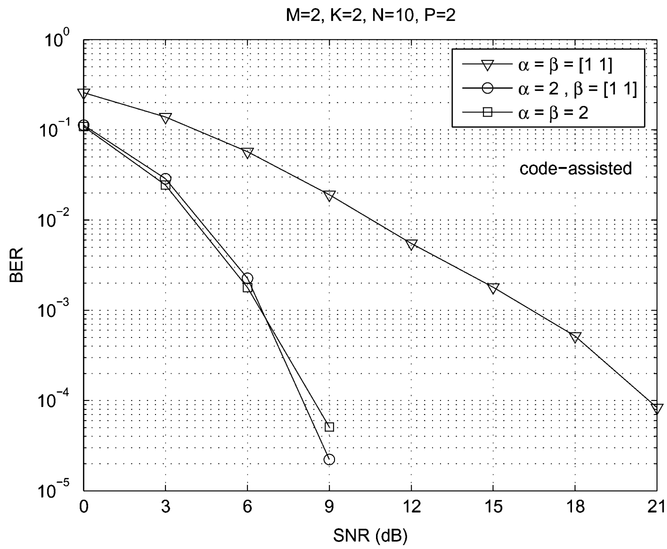

Fig. 3. Average performance of three different transmit schemes with $M = 2$.

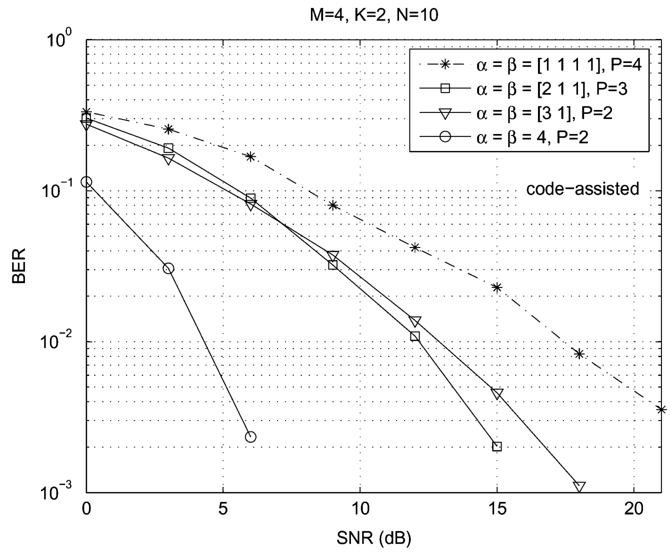

Fig. 4. Average performance of 4 different transmit schemes with $M = 4$.

at the top of each figure. We recall that for given $\boldsymbol{\alpha}$ and $\boldsymbol{\beta}$, the corresponding values of R and J can be deduced, as shown in Table I for $M = 4$.

It is worth mentioning that our simulation results do not distinguish between the detection of Q user signals with M_q transmit antennas, R_q data streams, and J_q spreading codes each, or the detection of a single-user signal with $M = M_1 + \cdots + M_Q$ antennas, $R = R_1 + \cdots + R_Q$ data streams and $J = J_1 + \cdots + J_Q$ spreading codes. Since the ALS receiver is based on a joint multiuser/multistream detection approach, distinguishing between both cases is not relevant for purposes of performance evaluation.

A. Performance of Different Schemes ($M = 2$ and $M = 4$)

First, we consider the code-assisted detection and investigate the performance of some multiple-antenna CDMA schemes for $M = 2$ and $M = 4$ transmit antennas. Fig. 3 depicts the performance of three different schemes for $M = 2$. Performance improves when going from full spatial multiplexing ($\boldsymbol{\alpha} = \boldsymbol{\beta} = [1\ 1]$) to full spatial spreading with code reuse ($\boldsymbol{\alpha} = \boldsymbol{\beta} = 2$). Note that such a performance gain comes at the expense of a reduction of the spectral efficiency by a factor of two. Spatial spreading with code multiplexing ($\boldsymbol{\alpha} = [2], \boldsymbol{\beta} = [1\ 1]$) offers nearly the same average performance as spatial spreading with code reuse. The use of code multiplexing in place of code reuse can be more attractive in scenarii where the spatial channels from the different transmit antennas are correlated and transmit spatial signatures are poor [32]. We shall come back to this issue latter. Fig. 4 shows the performance of four different schemes for $M = 4$, considering $R = J$ and $\boldsymbol{\alpha} = \boldsymbol{\beta}$. The spreading factor is adjusted to keep the spectral efficiency constant (except for $\boldsymbol{\alpha} = \boldsymbol{\beta} = 4$ where spectral efficiency is divided by two). A variable degree of spatial diversity is afforded by the different choices of $\boldsymbol{\alpha}$ and $\boldsymbol{\beta}$.

B. Influence of the Code Reuse Pattern (Choice of $\boldsymbol{\beta}$)

In Fig. 5, we compare the performance of two different schemes combining spatial spreading and spatial multiplexing

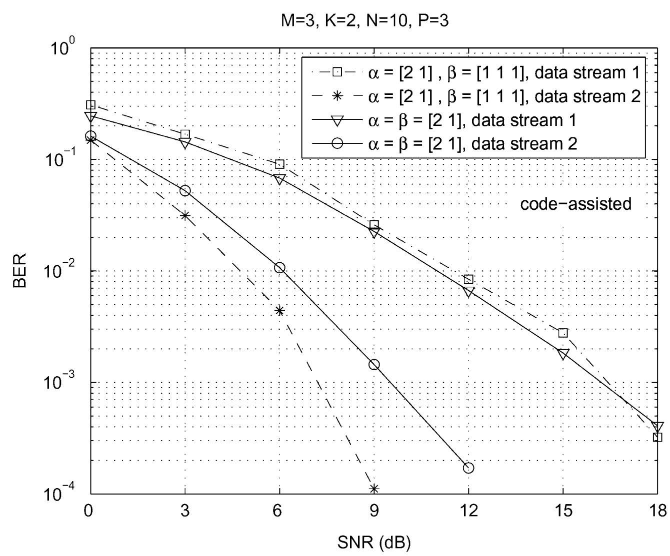

Fig. 5. Individual data stream performance for two different transmit schemes with $M = 3$ and different choices of $\boldsymbol{\beta}$.

for $M = 3$. Both schemes have the same spatial spreading pattern, the difference being on the code reuse/multiplexing pattern. In contrast to previous figures, we plot the individual performance for each data stream in order to verify the influence of code reuse/multiplexing. It can be concluded that the two transmit schemes mainly differ in the performance of the second data stream, which is significantly better as code multiplexing is used. This result confirms that using different codes for transmitting the same data stream across different antennas allows the receiver to use both spatial and code information to distinguish the transmitted substreams, corroborating with [2] and [32].

C. Performance Over Spatially-Correlated Channel

Now, we are interested in investigating the impact of using different codes for transmitting the same data stream over a

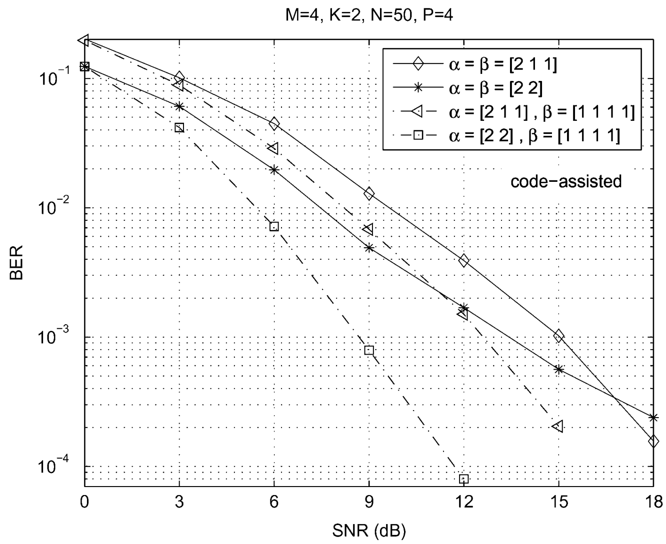

Fig. 6. Average performance of four different transmit schemes with $M = 4$ over a channel with transmit spatial correlation.

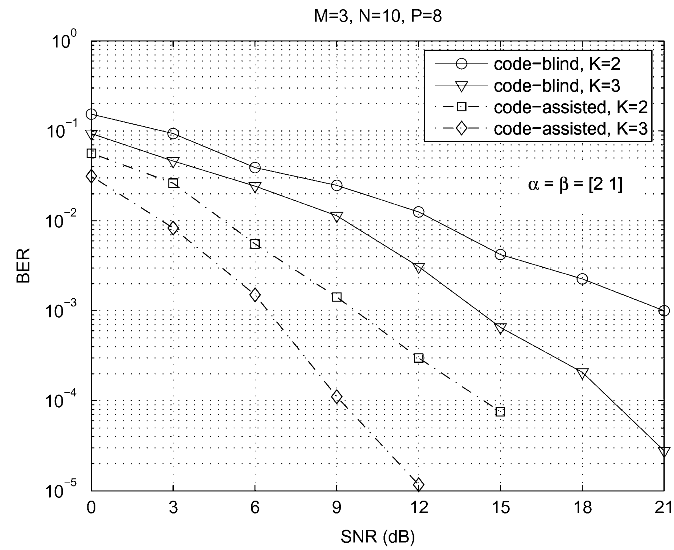

Fig. 7. Code-assisted versus code-blind detection with $M = 3$.

practical (nonideal) channel with transmit correlation. We assume that only the transmit antennas are correlated, which can be a reasonable assumption in uplink transmission with poor scattering around the transmitter. At the base-station receiver, we assume sufficient scattering so that the receive antennas are uncorrelated. We adopt the following channel model with transmit correlation [33]:

$$\mathbf{H} = \mathbf{H}_o \mathbf{R}_t^{1/2}$$

where $\mathbf{H}_o$ is a matrix of complex i.i.d. Gaussian variables of unity variance and $\mathbf{R}_t$ the transmit covariance matrix. In this experiment, we assume $M = 4$ and $\mathbf{R}_t$ is given by the matrix [34]

$$\mathbf{R}_t = \begin{bmatrix} 1 & 0.57e^{-2.25j} & 0.17e^{0.02j} & 0.29e^{-2.94j} \\ 0.57e^{2.25j} & 1 & 0.57e^{-2.25j} & 0.17e^{0.02j} \\ 0.17e^{-0.02j} & 0.57e^{2.25j} & 1 & 0.57e^{-2.25j} \\ 0.29e^{2.94j} & 0.17e^{-0.02j} & 0.57e^{2.25j} & 1 \end{bmatrix}.$$

We consider four allocation schemes having different spatial spreading/multiplexing and code reuse/multiplexing patterns. We focus on the isolated performance for each data stream. According to Fig. 6, for a fixed choice of $\boldsymbol{\alpha}$ and $\boldsymbol{\beta}$, better results are obtained when full code multiplexing is used ($\boldsymbol{\beta} = [1\ 1\ 1\ 1]$). Indeed, keeping $\boldsymbol{\alpha} = [2\ 2]$ and using $\boldsymbol{\beta} = [1\ 1\ 1\ 1]$ in place of $\boldsymbol{\beta} = [2\ 2]$, a significant performance improvement is obtained at the expense of using twice the number of spreading codes. The same comment is valid for $\boldsymbol{\alpha} = [2\ 1\ 1]$. Note that, when $\boldsymbol{\alpha} = \boldsymbol{\beta} = [2\ 2]$, the performance tends to saturate at high SNR as a consequence of transmit spatial correlation. These results show that the choice of the generating vectors is important in practical scenarii.

D. Code-Blind Versus Code-Assisted Detection

In all the previously obtained results, we have considered code-assisted detection by assuming perfectly orthogonal spreading codes (no interchip interference). The next results consider the more challenging code-blind detection, where the (effective) spreading codes are unknown to the receiver due to multipath propagation. The effective spreading codes are generated by convolving an orthogonal Hadamard code of length $P = 32$ chips with a two-tap multipath channel, the delay between the two taps being equal to two chip periods. At each run, these multipath components are drawn from an i.i.d. complex-valued Gaussian generator. Fig. 7 compares the performance of code-blind and code-assisted detection. In this case we use $\boldsymbol{\alpha} = \boldsymbol{\beta} = [2\ 1]$. We can observe a performance loss of the code-blind receiver with respect to the code-assisted one. The performance gap is attributed, in part, to the presence of inter-chip interference and the lack of knowledge of the code matrix which induces more parameters to be estimated by means of the ALS algorithm.

E. Comparison With the Optimum ZF Receiver

As a reference for comparison, we now consider the performance of the zero forcing (ZF) receiver with perfect knowledge of the channel and code matrices. The ZF receiver is compared with the channel- and code-blind ALS receiver. Using our notation, the ZF receiver consists in a single-step estimation of the symbol matrix given by

$$\hat{\mathbf{S}}_{\mathrm{ZF}}^T = [((\mathbf{C}\boldsymbol{\Phi}) \diamond \mathbf{H})\boldsymbol{\Psi}^T]^{\dagger} \tilde{\mathbf{X}}_2$$

$\mathbf{H}$ and $\mathbf{C}$ being perfectly known. We consider two allocation schemes with $\boldsymbol{\alpha} = \boldsymbol{\beta} = [2\ 1](M = 3)$ and $[2\ 2](M = 4)$. It can be seen from Fig. 8 that the gap between ALS and ZF is around 6 dB in terms of SNR, for a BER equal to $2 \cdot 10^{-2}$. We can observe that the same performance improvement is obtained for both ZF and ALS when M is increased.

VIII. Conclusion and Perspectives

This paper has proposed a new constrained tensor model for modeling multiple-antenna CDMA schemes with blind detection. The two constraint matrices of the tensor model (called *allocation matrices*) control the spatial spreading of the data

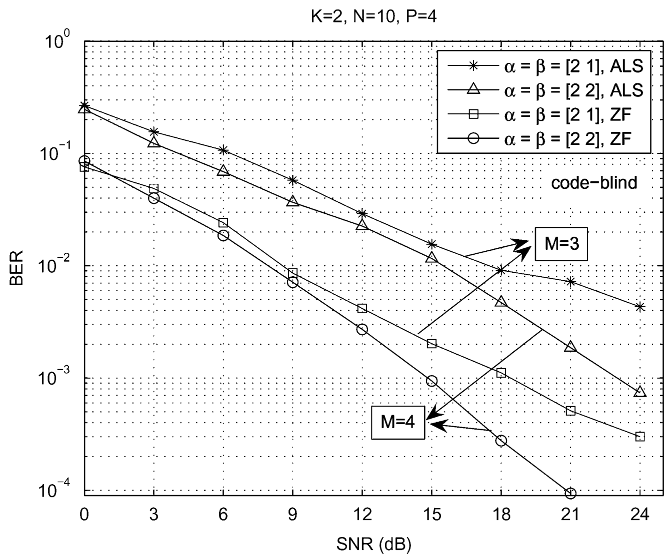

Fig. 8. Comparison between code-blind ALS and ZF receivers (with perfect channel/code knowledge for the ZF receiver).

streams and the spatial reuse of the spreading codes, respectively. By parameterizing these two allocation matrices by their corresponding generating vectors, we have presented a design procedure for systematically deriving a set of transmit schemes with guaranteed blind symbol recovery. The BER performance of several transmit schemes has been evaluated using the ALS algorithm. Simulation results have shown that remarkable performance is obtained with only two receive antennas and short data blocks. We emphasize that the introduction of the two allocation matrices into the multiple-antenna CDMA model can be further exploited. When some form of channel state information is available at the transmitter, the design of performance-optimized allocation matrices is an interesting issue to be investigated. For a fixed number M of transmit antennas, we could resort to limited feedback precoding [29], [30] to properly select the two allocation matrices from the finite-set of feasible choices (cf. Table I for $M = 4$).

Appendix

We demonstrate that the design criterion (20), which results in a partitioned structure for the canonical allocation matrices according to (21)–(22), leads to the uniqueness of $\mathbf{S}$ up to column permutation and scaling while the uniqueness of $\mathbf{C}$ exists up to multiplication by a nonsingular block-diagonal matrix and a block-diagonal permutation matrix.

Let us define $\mathbf{C} \doteq [\mathbf{C}_1, \ldots, \mathbf{C}_R] \in \mathbb{C}^{P \times J}$ and $\mathbf{C}_r \doteq [\mathbf{C}_{r,1}, \ldots, \mathbf{C}_{r,J_r}] \in \mathbb{C}^{P \times \alpha_r}$ with $\mathbf{C}_{r,j_r} \in \mathbb{C}^{P \times \beta_{r,j_r}}$, $j_r = 1, \ldots, J_r$, as the partitioned spreading code matrix. Let us also define $\mathbf{H} = [\mathbf{H}_1, \ldots, \mathbf{H}_R] \in \mathbb{C}^{K \times M}$ as the partitioned channel matrix. Based on these definitions, we can rewrite (13) in terms of this partitioning as

$$\mathbf{X}_{\cdot\cdot k} = \mathbf{S} \underbrace{\left(\sum_{r=1}^{R} \boldsymbol{\Psi}_r D_k \left(\mathbf{H}_r \right) \boldsymbol{\Phi}_r^T \right)}_{\bar{\mathbf{H}}_k} \mathbf{C}^T = \mathbf{S} \bar{\mathbf{H}}_k \mathbf{C}^T. \quad (27)$$

Due to the canonical structure of $\boldsymbol{\Psi}_r$ and $\boldsymbol{\Phi}_r$ defined in (21)–(22), it follows that $\bar{\mathbf{H}}_k$ is a row-wise block-diagonal matrix (it has only a single nonzero element per column), the blocks of which are row-vectors

$$\bar{\mathbf{H}}_k = \begin{bmatrix} \bar{h}_k^{(1,1)} & \cdots & \bar{h}_k^{(1,J_1)} & & & \mathbf{0} \\ & & & \ddots & & \\ & \mathbf{0} & & \bar{h}_k^{(R,1)} & \cdots & \bar{h}_k^{(R,J_R)} \end{bmatrix}$$

where

$$\bar{h}_k^{(r,j_r)} = \sum_{i=1}^{\beta_{r,j_r}} h_{k,\bar{\beta}_{r,j_{r-1}}+i}$$

with $\bar{\beta}_{r,j} = \sum_{i=1}^{j} \beta_{r,i}$. Let $\mathbf{T} \in \mathbb{C}^{R \times R}$, $\mathbf{U} \in \mathbb{C}^{J \times J}$ be nonsingular transformation matrices. Inserting $\mathbf{T}\mathbf{T}^{-1}$ and $\mathbf{U}\mathbf{U}^{-1}$ in (27) yields

$$\mathbf{X}_{\cdot\cdot k} = (\mathbf{S}\mathbf{T})(\mathbf{T}^{-1}\bar{\mathbf{H}}_k\mathbf{U}^{-T})(\mathbf{C}\mathbf{U})^T. \quad (28)$$

First, note that $\mathbf{T}^{-1}$ acts over the rows of $\bar{\mathbf{H}}_k$, while $\mathbf{U}^{-T}$ acts over the columns of $\bar{\mathbf{H}}_k$, respectively. It can be easily checked that $\mathbf{T}^{-1}$ only preserves the row-wise diagonal structure of $\bar{\mathbf{H}}_k$ if it is a diagonal matrix or a row-permutation of it, which leads to the form (23) of $\mathbf{T}$. On the other hand, any nonsingular matrix $\mathbf{U}^{-T}$ having a block-diagonal structure with blocks $\mathbf{U}_1 \in \mathbb{C}^{J_1 \times J_1}, \ldots, \mathbf{U}_R \in \mathbb{C}^{J_R \times J_R}$, preserves the structure of $\bar{\mathbf{H}}_k$ which implies a transformational ambiguity over the sets of $J_1, \ldots, J_R$ columns of $\mathbf{C}_1, \ldots, \mathbf{C}_R$. Note also that the blocks $\mathbf{U}_1, \ldots \mathbf{U}_R$ can be arbitrarily permuted without changing the pattern of zeros of $\bar{\mathbf{H}}_k$, which leads to the form (23) of $\mathbf{U}$.

The block-diagonal transformational ambiguity matrix $\mathbf{U} = \mathrm{blockdiag}(\mathbf{U}_1, \ldots, \mathbf{U}_R)$ exists when $J > R$ (more spreading codes than data streams). In the particular case $J = R$ (one-to-one correspondence between spreading codes and data streams) with $\alpha_r = \beta_r$, $r = 1, \ldots, R$, $\bar{\mathbf{H}}_k$ is reduced to a diagonal matrix and the joint uniqueness of $\mathbf{S}$ and $\mathbf{C}$ is achieved.

References

[1] G. L. Foschini and M. L. Gans, "On limits of wireless communications when using multiple antennas," *Wireless Pers. Commun.*, vol. 6, no. 3, pp. 311–335, 1998.
[2] H. Huang, H. Viswanathan, and G. J. Foschini, "Multiple antennas in cellular CDMA systems: Transmission, detection, and spectral efficiency," *IEEE Trans. Wireless Commun.*, vol. 1, no. 3, pp. 383–392, 2002.
[3] S. Sfar, R. D. Murch, and K. B. Letaief, "Layered spacetime multiuser detection over wireless uplink systems," *IEEE Trans. Wireless Commun.*, vol. 2, no. 4, pp. 653–668, Jul. 2003.
[4] L. Mailaender, "Linear MIMO equalization for CDMA downlink signals with code reuse," *IEEE Trans. Wireless Commun.*, vol. 4, no. 5, pp. 2423–2434, Sep. 2005.
[5] T. S. Dharma, A. S. Madhukumar, and A. B. Premkumar, "Layered space-time architecture for MIMO block spread CDMA systems," *IEEE Commun. Lett.*, vol. 10, no. 2, pp. 70–72, Feb. 2006.
[6] G. D. Golden, G. J. Foschini, R. A. Valenzuela, and P. W. Wolniansky, "Detection algorithm and initial laboratory results using the V-BLAST space-time communications architecture," *Electron. Lett.*, vol. 35, no. 7, pp. 14–15, Jan. 1999.
[7] B. Hochwald, T. L. Marzetta, and C. B. Papadias, "A transmitter diversity scheme for wideband CDMA systems based on space-time spreading," *IEEE J. Sel. Areas Commun.*, vol. 19, no. 1, pp. 48–60, Jan. 2001.

[8] R. Doostnejad, T. J. Lim, and E. Sousa, "Space-time spreading codes for a multiuser MIMO system," in *Proc. 36th Asilomar Conf. Signals, Syst. Comput.*, Pacific Grove, CA, Nov. 2002, pp. 1374–1378.

[9] R. Doostnejad, T. J. Lim, and E. Sousa, "Space-time multiplexing for MIMO multiuser downlink channels," *IEEE Trans. Wireless Commun.*, vol. 5, no. 7, pp. 1726–1734, Jul. 2006.

[10] L.-L. Yang, "MIMO-assisted space-code-division multiple-access: Linear detectors and performance over multipath fading channels," *IEEE J. Sel. Areas Commun.*, vol. 24, no. 1, pp. 121–131, Jan. 2006.

[11] N. D. Sidiropoulos, G. B. Giannakis, and R. Bro, "Blind PARAFAC receivers for DS-CDMA systems," *IEEE Trans. Signal Process.*, vol. 48, no. 3, pp. 810–822, Mar. 2000.

[12] N. D. Sidiropoulos and G. Z. Dimic, "Blind multiuser detection in WCDMA systems with large delay spread," *IEEE Signal Process. Lett.*, vol. 8, no. 3, pp. 87–89, Mar. 2001.

[13] A. de Baynast and L. De Lathauwer, "Dètection autodidacte pour des systèmes a accès multiple basèe sur 1'analyse PARAFAC," presented at the XIX GRETSI Symp. Signal Image Process., Paris, France, Sep. 2003.

[14] A. L. F. de Almeida, G. Favier, and J. C. M. Mota, "PARAFAC models for wireless communication systems," presented at the Int. Conf. Phys. Signal and Image Process. (PSIP), Toulouse, France, Jan. 31–Feb. 2 2005.

[15] A. L. F. de Almeida, G. Favier, and J. C. M. Mota, "PARAFAC-based unified tensor modeling for wireless communication systems with application to blind multiuser equalization," *Signal Process.*, vol. 87, no. 2, pp. 337–351, Feb. 2007.

[16] D. Nion and L. De Lathauwer, "A block factor analysis based receiver for blind multi-user access in wireless communications," presented at the ICASSP, Toulouse, France, May 2006.

[17] N. D. Sidiropoulos and R. Budampati, "Khatri-Rao space-time codes," *IEEE Trans. Signal Process.*, vol. 50, no. 10, pp. 2377–2388, Oct. 2002.

[18] A. de Baynast, L. De Lathauwer, and B. Aazhang, "Blind PARAFAC receivers for multiple access-multiple antenna systems," presented at the VTC Fall, Orlando, FL, Oct. 2003.

[19] A. L. F. de Almeida, G. Favier, and J. C. M. Mota, "Space-time multiplexing codes: A tensor modeling approach," presented at the IEEE Int. Workshop Signal Process. Adv. Wireless Commun. (SPAWC), Cannes, France, Jul. 2006.

[20] A. L. F. de Almeida, G. Favier, and J. C. M. Mota, "Tensor-based space-time multiplexing codes for MIMO-OFDM systems with blind detection," presented at the IEEE Int. Symp. Pers. Ind. Mob. Radio Commun. (PIMRC), Helsinki, Finland, Sep. 11–14, 2006.

[21] R. Bro, "Multi-way analysis in the food industry: models, algorithms and applications," Ph.D. dissertation, Univ. Amsterdam, Amsterdam, The Netherlands, 1998.

[22] H. A. Kiers and A. K. Smilde, "Constrained three-mode factor analysis as a tool for parameter estimation with second-order instrumental data," *J. Chemometr.*, vol. 12, no. 2, pp. 125–147, Dec. 1998.

[23] J. M. F. ten Berge, "Non-triviality and identification of a constrained Tucker3 analysis," *J. Chemometr.*, vol. 16, pp. 609–612, 2002.

[24] L. R. Tucker, "Some mathematical notes on three-mode factor analysis," *Psychometrika*, vol. 31, pp. 279–311, 1966.

[25] R. Bro, R. A. Harshman, and N. D. Sidiropoulos, "Modeling multi-way data with linearly dependent loadings," Univ. of Denmark, Denmark, KVL Tech. Rep. 176, 2005.

[26] Z. Xu, P. Liu, and X. Wang, "Blind multiuser detection: From MOE to subspace methods," *IEEE Trans. Signal Process.*, vol. 52, no. 2, pp. 91–103, Feb. 2004.

[27] R. A. Harshman, "Foundations of the PARAFAC procedure: Model and conditions for an "explanatory" multi-mode factor analysis," *UCLA Working Papers in Phonet.*, vol. 16, pp. 1–84, Dec. 1970.

[28] G. E. Andrews*, The Theory of Partitions*. Cambridge, U.K.: Cambridge Univ. Press, 1984.

[29] R. W. Heath and D. J. Love, "Multimode antenna selection for spatial multiplexing systems with linear receivers," *IEEE Trans. Signal Process.*, vol. 53, no. 8, pp. 3042–3056, Aug. 2005.

[30] D. J. Love and R. W. Heath, "Multimode preceding for MIMO wireless systems," *IEEE Trans. Signal Process.*, vol. 53, no. 10, pp. 3674–3687, Oct. 2005.

[31] N. D. Sidiropoulos and X. Liu, "Cramer-Rao bounds for low-rank decomposition of multidimensional arrays," *IEEE Trans. Signal Process.*, vol. 49, no. 9, pp. 2074–2086, Sep. 2001.

[32] S. Mudulodu and A. J. Paulraj, "A simple multiplexing scheme for MIMO systems using multiple spreading codes," in *Proc. 34th ASILOMAR Conf. Signals, Syst. Comput.*, Pacific Grove, CA, Oct. 29—Nov. 1 2000, vol. 1, pp. 769–774.

[33] D. Shiu, G. J. Foschini, M. J. Gans, and J. M. Kahn, "Fading correlation and its effect on the capacity of multi-element antenna systems," *IEEE Trans. Commun.*, vol. 48, no. 3, pp. 502–513, 2000.

[34] D. A. Gore, R. W. Heath, Jr., and A. J. Paulraj, "Transmit selection in spatial multiplexing systems," *IEEE Commun. Lett.*, vol. 6, no. 11, pp. 491–493, 2002.

André L. F. de Almeida was born in Teresina, Brazil, in 1978. He received the B.Sc. and M.Sc. degrees in electrical engineering from the Federal University of Ceará, Brazil, in 2001 and 2003, respectively, and the double Ph.D. degree in science and teleinformatics engineering from the University of Nice, Sophia Antipolis, France, and the Federal University of Ceará, Fortaleza, Brazil, in 2007.

He is currently a Postdoctoral Fellow with the I3S Laboratory, Sophia Antipolis. He is also affiliated to the Department of Teleinformatics Engineering of the Federal University of Ceará as an Associated Researcher with the Wireless Telecom Research Group. His research interest lies in the area of signal processing for communications, and include array processing, blind signal separation and equalization, multiple-antenna techniques, and multicarrier and multiuser communications. He has focused on the development of tensor decompositions with applications in MIMO wireless communication systems.

Gérard Favier was born in Avignon, France, in 1949. He received the engineering diplomas from the Ecole Nationale Supérieure de Chronométrie et de Micromécanique (ENSCM), Besançon, France, and Ecole Nationale Supérieure de l'Aéronautique et de l'Espace (ENSAE), Toulouse, France, in 1973 and 1974, respectively. He received the Engineering Doctorate and State Doctorate degrees from the University of Nice, Sophia Antipolis, in 1977 and 1981, respectively.

In 1976, he joined the Centre National de la Recherche Scientifique (CNRS) where he now works as a Research Director of CNRS, I3S Laboratory, Sophia Antipolis. From 1995 to 1999, he was the Director of the I3S Laboratory. His present research interests include nonlinear process modelling and identification, blind equalization, tensor decompositions, and tensor approaches for wireless communication systems.

João Cesar M. Mota was born in Rio de Janeiro, Brazil, in 1954. He received the B.Sc. degree in physics from the Universidade Federal do Ceará (UFC), Brazil, in 1978, the M.Sc. degree from Pontifícia Universidade Católica (PUC-RJ), Brazil, in 1984, and the Ph.D. degree from the Universidade Estadual de Campinas—UNICAMP, Brazil, in 1992, all in telecommunications engineering.

Since August 1979, he has been with the UFC, and currently is Professor with the Teleinformatics Engineering Department. He was with the Institut National des Télécommunications and Institut de Recherche en Communications et Cybernetique de Nantes, both in France, as an Invited Professor during 1996–1998 and spring 2006, respectively. His research interests include digital communications, adaptive filter theory, and signal processing.

Dr. Mota was General Chairman of the 19th Brazilian Telecommunications Symposium—SBrT'2001 and the International Symposium on Telecommunications—ITS'2006. He is responsible for the international mobility program for engineering students of UFC. He is a member and counselor of the Sociedade Brasileira de Telecomunicaões, and a member of the IEEE Communications Society and IEEE Signal Processing Society. He is a counselor of the IEEE Student Branch in UFC.